Drug Design, Development and Therapy

Dovepress
open access to scientific and medical research

Open Access Full Text Article

ORIGINAL RESEARCH

Timosaponin B-II ameliorates diabetic nephropathy via TXNIP, mTOR, and NF-κB signaling pathways in alloxan-induced mice

This article was published in the following Dove Press journal:
Drug Design, Development and Therapy
27 November 2015
Number of times this article has been viewed

Yong-Liang Yuan[1,*]
Chang-Run Guo[1,*]
Ling-Ling Cui[1]
Shi-Xia Ruan[1]
Chun-Feng Zhang[1]
De Ji[2]
Zhong-Lin Yang[1]
Fei Li[1]

[1]State Key Laboratory of Natural Medicines, China Pharmaceutical University, [2]College of Pharmacy, Nanjing University of Chinese Medicine, Nanjing, People's Republic of China

*These authors contributed equally to this work

Background: Many synthesized drugs with clinical severe side effects have been used for diabetic nephropathy (DN) treatment. Therefore, it is urgent and necessary to identify natural and safe agents to remedy DN. Timosaponin B-II (TB-II), a major steroidal saponin constituent in *Anemarrhena asphodeloides* Bunge, exhibits various activities, including anti-inflammatory and hypoglycemic functions. However, the anti-DN effects and potential mechanism(s) of TB-II have not been previously reported.

Purpose: To investigate the effect of TB-II on DN in alloxan-induced diabetic mice.

Methods: TB-II was isolated and purified from *A. asphodeloides* Bunge using macroporous adsorption resin and preparative high-performance liquid chromatography. The effect of TB-II on DN was evaluated in alloxan-induced diabetic mice using an assay kit and immunohistochemical determination in vivo. The expression of mammalian target of rapamycin (mTOR), thioredoxin-interacting protein (TXNIP), and nuclear transcription factor-κB (NF-κB) signaling pathways was also measured using Western blot analysis.

Results: TB-II significantly decreased the blood glucose levels and ameliorated renal histopathological injury in alloxan-induced diabetic mice. In addition, TB-II remarkably decreased the levels of renal function biochemical factors, such as kidney index, blood urea nitrogen, serum creatinine, urinary uric acid, urine creatinine, and urine protein, and it reduced lipid metabolism levels of total cholesterol and triglycerides and the levels of inflammatory cytokines interleukin-6 and tumor necrosis factor-α in alloxan-induced mice. Furthermore, TB-II inhibited the expression of mTOR, TXNIP, and NF-κB.

Conclusion: The results revealed that TB-II plays an important role in DN via TXNIP, mTOR, and NF-κB signaling pathways. Overall, TB-II exhibited a prominently ameliorative effect on alloxan-induced DN.

Keywords: *Anemarrhena asphodeloides* Bunge, timosaponin B-II, diabetic nephropathy, TXNIP, mTOR, NF-κB

Introduction

Diabetes mellitus is a chronic metabolic disease characterized by high levels of blood glucose resulting from the impaired secretion of insulin, insulin insensitivity, and inflammation response.[1–3] According to the latest estimates, the diabetes mellitus population will be up to 591.9 million persons by the year 2035.[4] Diabetes has been identified as the third serious chronic disease to human health after cardiovascular disease and cancer. Long-term hyperglycemia affects many tissues and organs of the body, leading to various diabetic chronic complications, such as nephropathy,[5] neuropathy,[6] and retinopathy.[7] Diabetic nephropathy (DN) is one of the most common diabetic complications, developing in approximately 30% of diabetic patients, which

Correspondence: Zhong-Lin Yang; Fei Li
State Key Laboratory of Natural Medicines, China Pharmaceutical University, 24 Tongjia Lane, Nanjing 210009, People's Republic of China
Tel +86 25 8327 1425; +86 25 8327 1382
Email yzl1950@126.com; lifeicpu@163.com

might initially develop into nephrotic syndrome, eventually leading to kidney failure and death.[8] The characteristics of renal injury include renal hypertrophy and changes of biochemical features, such as kidney index (KI), blood urea nitrogen (BUN), serum creatinine (SCr), serum uric acid (SUA), serum triglycerides (TG), total cholesterol (TC), urinary uric acid (UUA), urine creatinine (UCr), and urine protein. Furthermore, recent studies have clearly shown that inflammation promotes the occurrence of DN.[2,9]

The production of inflammatory factors, tumor necrosis factor-α (TNF-α) and interleukin-6 (IL-6), was stimulated via the nuclear transcription factor-κB (NF-κB) pathway, whereby IκB kinase-β activates inhibitor of nuclear factor kappa-B (IκB) through phosphorylation.[1,10] In addition, the expression of thioredoxin-interacting protein (TXNIP) plays an important role in the occurrence and development of DN[11,12] and the expression of mammalian target of rapamycin (mTOR) pathways.[13] Currently, chemically synthesized drugs, with many side effects, are clinically used for DN treatment. Therefore, it is necessary and urgent to search natural and safe agents to remedy DN. The rhizomes of *Anemarrhena asphodeloides* Bunge, referred to as *zhi mu* in Chinese, is a traditional Chinese medicine used to treat arthralgia, hematochezia, bone-steaming, cough, and hemoptysis and has also been used as an ingredient of healthy food, wine, tea, and biological toothpaste.[14] The chemical components isolated from *A. asphodeloides* Bunge include steroidal saponins, flavonoids, alkaloids, steroids, organic acids, anthraquinones, and others.[14] The steroidal saponins comprise more than 6% of the rhizome.[15] Timosaponin B-II (TB-II) is a major steroidal saponin constituent of *A. asphodeloides* Bunge. The structure of TB-II is shown in Figure 1. A recent study showed that TB-II exhibits various pharmacological features, such as anti-dementia,[16] antidepression,[17] and anti-inflammatory properties,[18] cardioprotective effects,[19] and antiplatelet and antithrombotic activities.[20] Although the hypoglycemic activity of TB-II has been previously reported,[21] reports regarding the mechanism(s) of lowering blood glucose are limited. Thus, the aim of the present study was to examine the effect of TB-II on alloxan-induced renal injury and determine the potential underlying mechanism(s) in alloxan-induced mice. The workflow of the present study is shown in Figure S1.

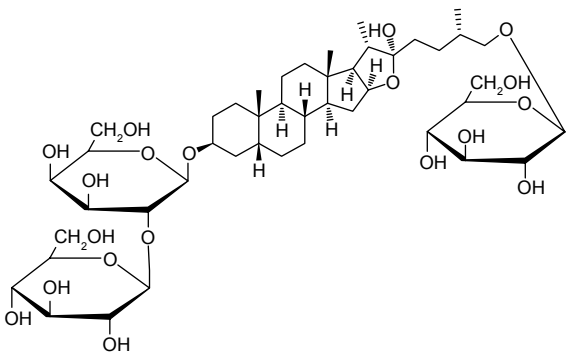

Figure 1 The structural formula of TB-II.
Abbreviation: TB-II, timosaponin B-II.

Materials and methods

Chemicals and reagents

Rosiglitazone (ROG, 1 mg/pill) was purchased from the Chengdu Hengrui Pharmaceutical Co. (Chengdu, People's Republic of China). Alloxan was purchased from the Sigma-Aldrich Chemical Co. (St Louis, MO, USA). Commercial reagent kits, including BUN, SCr, UUA, UCr, urine protein, TC, TG, TNF-α, and IL-6, were purchased from the Nanjing Jiancheng Bioengineering Institute (Nanjing, People's Republic of China). All chemical reagents used in the present study were purchased from Nanjing Chemical Reagent Co., Ltd (Nanjing, People's Republic of China). Primary antibodies against phospho-NF-κBp65, NF-κBp65, phospho-IκB, IκB, TXNIP, phospho-mTOR, mTOR, and glyceraldehyde 3-phosphate dehydrogenase (GAPDH) were obtained from Cell Signaling Technology Inc. (Beverly, MA, USA).

Plant material and preparation of TB-II

Dried *A. asphodeloides* Bunge rhizomes were purchased from the Hebei Anguo Pharmaceutical Group Co. (Shijiazhuang, People's Republic of China), and Prof Lian-Wen Qi (State Key Laboratory of Natural Medicines, China Pharmaceutical University, Nanjing, People's Republic of China) subsequently identified the sample. The sample (No 20141226) was stored in a laboratory at Traditional Chinese Medicine of China Pharmaceutical University.

The *A. asphodeloides* Bunge rhizomes (1.0 kg) were re-extracted twice using 96% ethanol at 85°C (2 hours each). The extracts were vacuum-dried (55°C) to collect the ethanol using a rotary evaporation instrument. The crude extract was obtained (103 g, 10.1%, w/w) and dissolved in distilled water (5 L), followed by filtration, and the resulting filtrates were pooled. After filtration, the filtrate was loaded onto HPD100 macroporous resin (10×100 cm) at a flow rate of 20 mL/min with a step gradient of 20% ethanol, and the 40% ethanol effluent was subsequently collected. The effluent was initially vacuum-dried (55°C) and subsequently moved to a vacuum oven for further drying. Semi-preparative high-performance liquid chromatography (pre-HPLC) was performed using an ODS C18 chromatographic column (10×250 mm, 5 μm) to

purify the dried sample containing TB-II. The mobile phase comprised acetonitrile and deionized water (30/70, v/v) at a flow rate of 1.0 mL/min. The effluent containing TB-II was pooled and vacuum-dried (55°C) to obtain high-purity TB-II.

Identification of TB-II and quantitative determination

The purity of the TB-II sample was authenticated using HPLC-MS-Q-TOF, ^{1}H-NMR, and ^{13}C-NMR (Table S1, Figure S2 and S3). The quantitation of TB-II was analyzed through HPLC using a C18 analytical column (Agilent Technologies, Santa Clara, CA, USA) equipped with an evaporative light-scattering (ELSD) detector at a flow rate of 1.0 mL/min. The mobile phase comprised acetonitrile and distilled water (v/v, 25:75). Approximately 10 μL of TB-II (0.5 mg/mL) was injected into an HPLC column to measure the purity of the sample (purity 97%, HPLC, Figure S2).

Animals

Male ICR mice (n=50, with body weight of 21±2 g) were obtained from the Laboratory Animal Center at Nantong University (Nantong, People's Republic of China, NO SCKX2008-0010), and the animals were caged with free food and water under a 12-hour light/dark control cycle. All animal experimentation protocols were performed according to guidelines of China Pharmaceutical University and approved by the Animal Care & Ethics Committee of China Pharmaceutical University.

Experimental design

After acclimatization for 1 week, the ICR mice were randomly divided into two groups: a natural control (NC) group (n=10) and an alloxan-induced group (n=40), and the alloxan-induced group was administered a single tail intravenous injection with alloxan (60 mg/kg, diluted with natural saline). On the third day, the alloxan-induced group was randomly assigned into four groups: the model group (n=10), diabetic mice treated with natural saline; the ROG group (n=10), diabetic mice administered ROG 10 mg/kg/day; the TB-II low-dose treatment group (n=10), diabetic mice administered TB-II 50 mg/kg/day; and the TB-II high-dose treatment group (n=10), diabetic mice administered TB-II 100 mg/kg/day.

All groups were orally administered an equal volume of distilled water or different samples between 9 am and 10 am every morning for 4 weeks. Urine samples were collected from mice in metabolic cages at 24 hours prior to the end of the experiment, and blood samples were collected from the retro-orbital venous plexus. Subsequently, the animals were sacrificed, and the kidneys were rapidly excised and weighed. The left kidneys were fixed in 10% buffered formalin for histological analysis, while the right kidney tissues were immediately frozen in liquid nitrogen for the subsequent analysis of the cytokine levels and western blotting.

Analysis of blood and urine samples

The blood was clotted and centrifuged at 4,000× *g* for 10 minutes, and serum was isolated. The blood glucose, SCr, BUN, TC, and TG levels were determined using commercially available kits according to the manufacturer's instructions. Similarly, the urine samples were centrifuged at 4,000× *g* for 10 minutes to obtain the supernatant. The UUA, UCr, and urine protein concentrations were determined using enzyme-linked immunosorbent assay (ELISA) kits.

Histological examination

The tissues were processed for histopathological assessment as previously reported.[22,23] For immunohistochemical staining, the renal samples were fixed in 10% neutral-buffered formalin for routine dehydration, followed by embedding in paraffin, sectioning (4 μm slices), and mounting onto microscope slides. An investigator, blinded to the origin of the sections, assessed at least 25 random glomeruli from each section under an electron microscope (magnification ×400).

Analysis of cytokine levels in kidney tissues

The IL-6 and TNF-α concentrations in the renal homogenates were measured using commercial ELISA kits according to the manufacturer's instructions.

Western blot analysis

The kidney tissues were homogenized, and subsequently lysed in radioimmunoprecipitation assay (RIPA) lysis buffer containing 50 mM Tris-HCl (pH 7.5), 0.1% sodium dodecylsulfate (SDS), 150 mM NaCl, 1% NP-40, 0.5% deoxycholic acid, 1 mM ethylenediaminetetraacetic acid (EDTA), 1 mM ethylene glycol tetraacetic acid (EGTA), 1 mM Na_3VO_4, 1% Triton x-100, 1 mg/mL aprotinin, 1 mg/mL leupeptin, and 0.5 mM phenylmethylsulfonyl fluoride. Subsequently, the kidney lysates were centrifuged at 12,000× *g* at 4°C for 30 minutes to obtain a supernatant containing cellular proteins. The same amounts of protein from each sample were isolated through SDS-polyacrylamide gel electrophoresis, loaded in the lane, transferred onto the polyvinylidene difluoride membranes, blocked for 1 hour at room temperature with 5% skim milk,

and subsequently probed at 4°C overnight with the following primary antibodies: phospho-mTOR, phospho-NF-κBp65, phospho-inhibitory kappa B alpha (IκBα), mTOR, TXNIP, NF-κBp65, IκBα, and GAPDH. After rinsing three times with tris-buffered saline and tween 20, the membranes were probed with secondary antibody for 1 hour at room temperature according to the manufacturer's instructions. The protein bands were visualized using an enhanced chemiluminescence reagent (Millipore, Billerica, MA, USA). The intensity of the bands was scanned and quantified using the image analysis software ImageJ (NIH Image analysis software v1.46 [National Institute of Mental Health, MD, USA]).

Statistical analysis

Data were expressed as the means ± standard error of the mean (SEM). The statistical analysis was performed using one-way analysis of variance followed by Tukey's post hoc test for multiple comparisons. In all cases, $P<0.05$ was considered significant.

Results

Electrospray ionization mass spectrometry and nuclear magnetic resonance (Figures S3 and S4) were used to reveal the structure of TB-II, identified as (25*S*)-3β-[(2-*O*-β-D-glucopyranosyl-β-D-galactopyranosyl)oxy]-26-(β-D-glucopyranosyloxy)-5β-furostane-22-ol.

As shown in Figure 2, the blood glucose levels in alloxan-induced mice significantly increased to 21.15 mmol/L compared with 5.62 mmol/L in the normal control group ($P<0.001$). Nevertheless, after treatment with ROG (10 mg/kg) and TB-II (50 and 100 mg/kg), the blood glucose levels were notably decreased to 7.19, 13.53, and 7.92 mmol/L, respectively ($P<0.01$ vs the normal control group). The TB-II (100 mg/kg) group showed a similar effect of regulating the blood glucose level compared with ROG group.

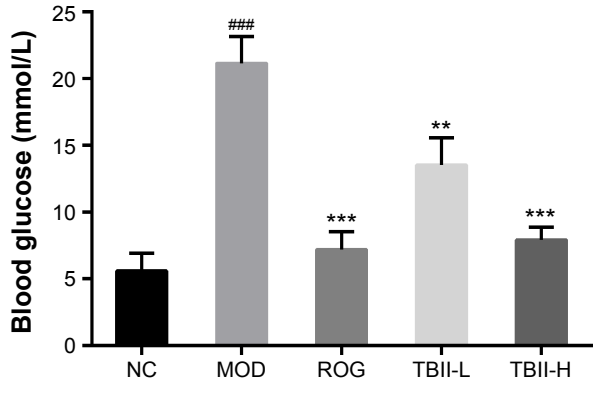

Figure 2 Effect of TB-II on blood glucose levels in diabetic mice.
Notes: The values are presented as the means ± SD (n=10). ###$P<0.001$ vs the normal control group; **$P<0.01$, ***$P<0.01$ vs the diabetic control group.
Abbreviations: MOD, model group; NC, natural control group; ROG, rosiglitazone treatment group; TBII-L, TB-II low-dose treatment group; TBII-H, TB-II high-dose treatment group; TB-II, timosaponin B-II; SD, standard deviation.

The levels of KIs, including SCr, BUN, UUA, UCr, and urine protein, were associated with renal injury. As illustrated in Figure 3, the KIs, SCr, and BUN were exceedingly increased in the diabetic model control group vs the normal control group ($P<0.001$). Treatment with TB-II (50 and 100 mg/kg) and ROG (10 mg/kg) notably reduced the increased KI compared with the diabetic model control group ($P<0.001$), including BUN and SCr levels ($P<0.001$). In contrast, there was no significant difference between TB-II (50 and 100 mg/kg) and ROG (10 mg/kg) in KI, BUN, and SCr levels. In addition, the excretion of UUA, UCr, and urine protein indicated glomerular dysfunction. The significantly increased levels of UUA, UCr, and urine protein in the diabetic model control group were compared with the normal control group ($P<0.001$). Treatment with TB-II (50 and 100 mg/kg) and ROG (10 mg/kg) for 4 weeks markedly decreased the elevated levels of UUA, UCr, and urine protein vs the diabetic model control group, respectively ($P<0.001$, <0.01). In addition, there was no significant difference between TB-II (50 and 100 mg/kg) and ROG (10 mg/kg) in the levels of UUA, UCr, and urine protein.

As shown in Figure 4, the levels of TC and TG were markedly higher in the diabetic control group compared with the NC group, respectively ($P<0.001$). However, treatment with TB-II at the doses of 50 and 100 mg/kg and ROG (10 mg/kg) for 4 weeks observably decreased the elevated TC and TG levels vs the diabetic model control group ($P<0.01$). In contrast, the TB-II (100 mg/kg) group showed similar regulation of the TC and TG levels compared with the ROG group.

As shown in Figure 5, the levels of IL-6 and TNF-α markedly increased in the diabetic control group vs the NC group ($P<0.001$), respectively. Importantly, after pretreatment with TB-II (50 and 100 mg/kg) and ROG (10 mg/kg), the levels of IL-6 and TNF-α were obviously higher than those in the diabetic model control group, respectively ($P<0.001$). However, after treatment with TB-II (100 mg/kg) similar levels of IL-6 and TNF-α were observed compared with ROG (10 mg/kg) treatment in diabetic mice.

The histopathological examination of the kidneys of normal control mice revealed that the kidney samples were normal and clear. There were no pathological changes of glomerular, no nodular sclerosis, no thickening of the glomerular basement membrane (GBM) and no mesangial matrix proliferate (Figure 6A). Representative changes were

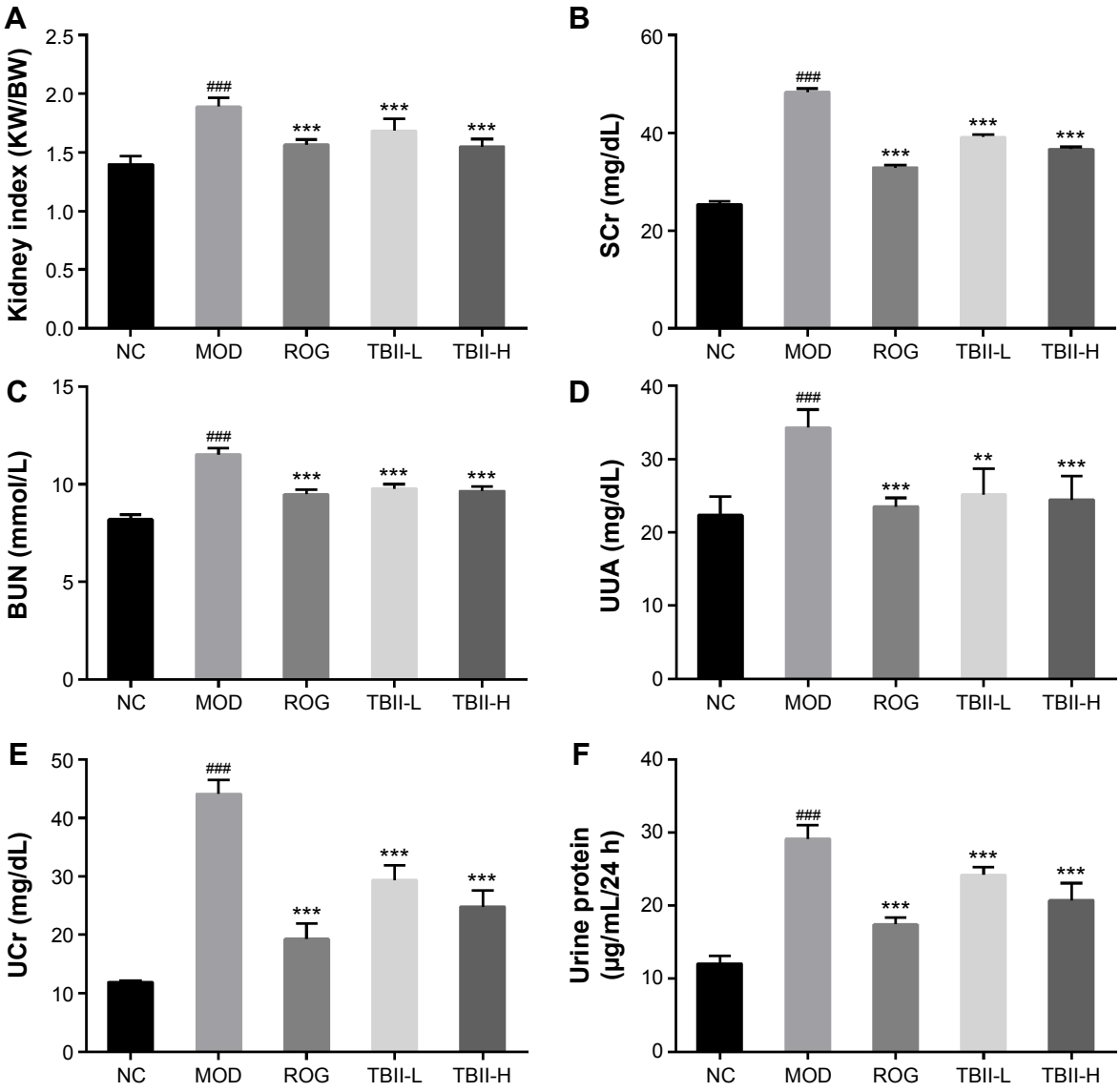

Figure 3 Effects of TB-II on KI (**A**), SCr (**B**), BUN (**C**), UUA (**D**), UCr (**E**), and urine protein (**F**).
Notes: The values are expressed as the means ± SD (n=10). ###$P<0.001$ vs the normal control group; **$P<0.01$, ***$P<0.01$ vs the diabetic control group.
Abbreviations: BUN, blood urea nitrogen; KI, kidney index; NC, natural control group; MOD, model group; ROG, rosiglitazone treatment group; SCr, serum creatinine; TBII-L, TB-II low-dose treatment group; TBII-H, TB-II high-dose treatment group; UUA, urinary uric acid; UCr, urine creatinine; TB-II, timosaponin B-II; SD, standard deviation.

observed in the kidneys of the diabetic control mice. The sections obtained from diabetic model control mice showed signs of thickened GBM, the glomerulus hypertrophy, mesangial matrix proliferate, and nodular sclerosis (Figure 6B). The sections obtained from diabetic model control mice showed signs of thickened basement membranes, tubular necrosis, and glomeruli. However, treatment with TB-II (50 and 100 mg/kg) for 4 weeks significantly inhibited the changes observed in the kidneys (Figure 6D and E) and the ROG-treated group (Figure 6C).

As shown in Figure 7A and B, the levels of p-NF-κBp65, p-1κBα in the diabetic control group were upregulated in contrast with the normal group and the expression levels of NF-κBp65, IκBα were used as inner controls ($P<0.001$). In contrast, treatment with TB-II (50, 100 mg/kg) and ROG (10 mg/kg) significantly decreased the levels of p-NF-κBp65/NF-κBp65, p-1κBα/1κBα vs the diabetic model control group ($P<0.001$). As illustrated in Figure 7C, Western blot analysis of the diabetic control group displayed downregulated levels of p-mTOR in contrast with the normal group, and mTOR expression levels were used as inner controls ($P<0.001$). Treatment with TB-II at 100 mg/kg for 4 weeks significantly inhibited the downregulated levels of p-mTOR/mTOR vs the diabetic model control group. In contrast, the levels of TXNIP in the diabetic model control group were upregulated compared with the normal group, and GAPDH expression levels

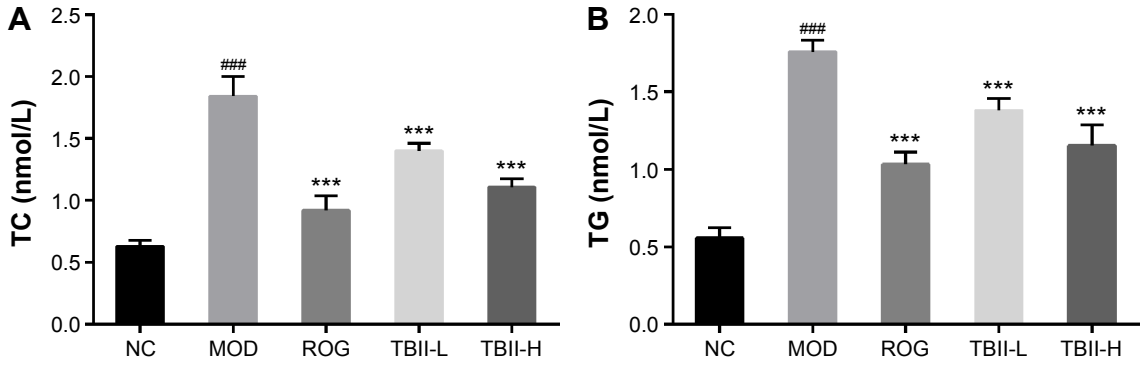

Figure 4 The effects of TB-II on TC (**A**) and TG (**B**). The TC and TG concentrations in conditioned medium were measured using ELISA kits.
Notes: The values are expressed the means ± SD (n=10). ###$P<0.001$ vs the normal control group; ***$P<0.001$ vs the diabetic control group.
Abbreviations: MOD, model group; NC, natural control group; ROG, rosiglitazone treatment group; TBII-L, TB-II low-dose treatment group; TBII-H, TB-II high-dose treatment group; TC, total cholesterol; TG, triglycerides; TB-II, timosaponin B-II; SD, standard deviation; ELISA, enzyme-linked immunosorbent assay.

were used as inner controls ($P<0.001$, Figure 7D). Notably, treatment with TB-II (50 and 100 mg/kg) and ROG (10 mg/kg) for 4 weeks significantly decreased the upregulated levels of TXNIP/GAPDH in the diabetic mice ($P<0.001$).

Discussion

In previous studies, TB-II exhibited an anti-inflammatory effect and hypoglycemic activity,[18,21] suggesting that TB-II shows potential as a DN treatment via anti-inflammatory effects. Therefore, this study investigated the anti-DN effect of TB-II and the related underlying mechanisms.

Alloxan, a model diabetes agent, induced diabetic renal changes and nephrotoxic alterations.[24,25] Thus, alloxan-induced diabetes was selected as a model for the renal injury status in diabetic mice. Generally, ROG was used as a thiazolidinedione class of antidiabetic drugs with antidiabetic and anti-inflammatory effects via the NF-κB pathway in patients.[26,27] Therefore, ROG represents an appropriate positive control. The results of the present study indicated that alloxan-induced diabetic mice showed markedly elevated levels of blood glucose. In contrast, both ROG and TB-II groups significantly decreased the blood glucose levels in diabetic mice, suggesting that TB-II exhibits potential antidiabetic activities similar to ROG.

Renal hypertrophy, nodular sclerosis, thickening of the GBM and no mesangial matrix proliferate are the typical hallmarks of diabetic renal injury. In the present study, the diabetic mice demonstrated these features; however, TB-II treatment ameliorated the suppression of nodular sclerosis and alleviated glomerular injuries.

Increasing evidence showed that uric acid levels gradually increased with the progression of DN, suggesting that hyperuricemia might accelerate the occurrence and development of type 2 DN in patients.[28] Lowering serum uric acid levels could slow the progression of renal disease.[29] The indices of uric acid excretion include SCr, BUN, UUA, and UCr.[30] In the present study, TB-II significantly decreased SCr, BUN, UUA, UCr, and urine protein in alloxan-induced diabetic mice, suggesting that TB-II partially restores diabetic renal injury.

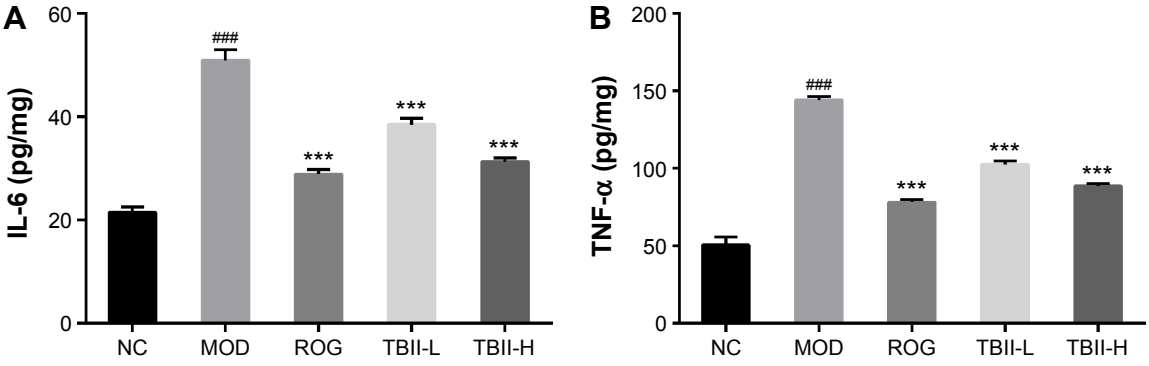

Figure 5 TB-II inhibited on IL-6 (**A**) and TNF-α (**B**) production in diabetic mice. The TNF-α and IL-6 concentrations in conditioned medium were measured using ELISA kits.
Notes: The values are expressed as the means ± SD (n=10). ###$P<0.001$ vs the normal control group; ***$P<0.001$ vs the diabetic control group.
Abbreviations: IL-6, interleukin-6; MOD, model group; NC, natural control group; ROG, rosiglitazone treatment group; TBII-L, TB-II low-dose treatment group; TBII-H, TB-II high-dose treatment group; TNF, tumor necrosis factor-α; TB-II, timosaponin B-II; SD, standard deviation; ELISA, enzyme-linked immunosorbent assay.

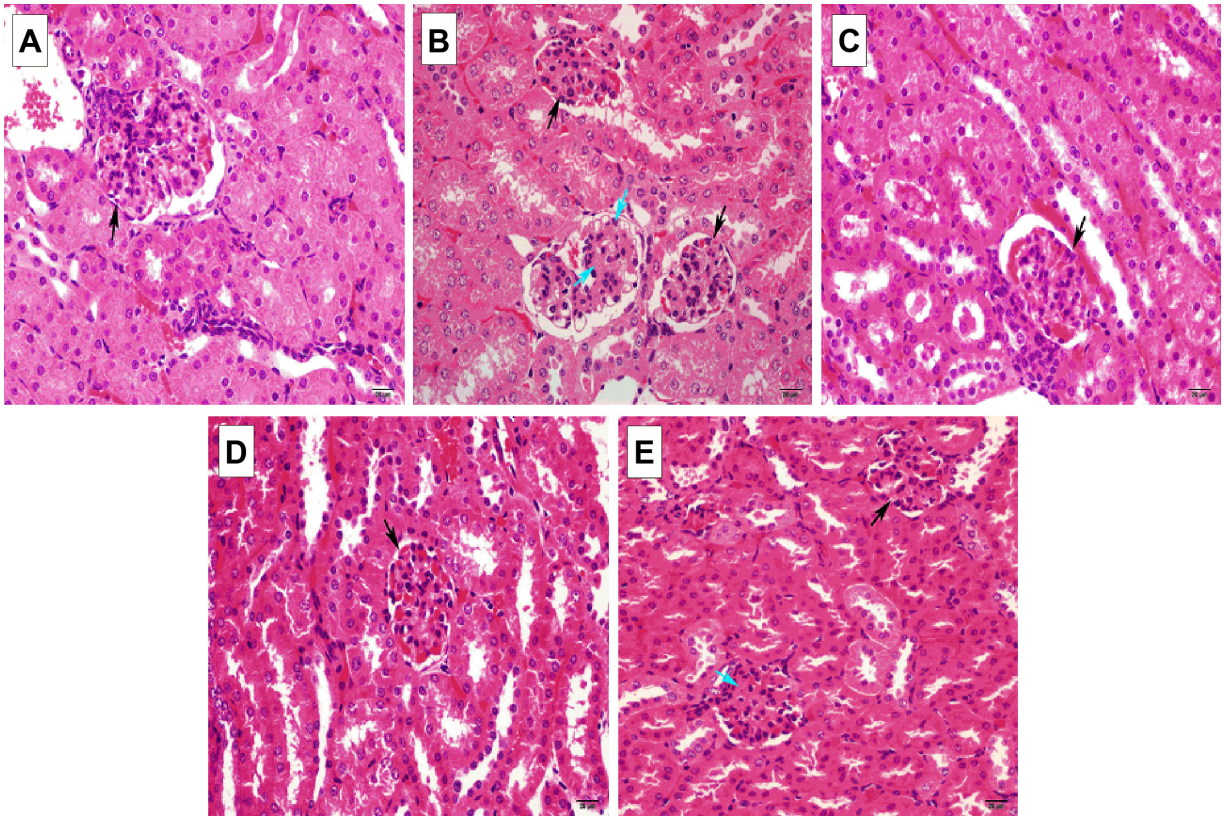

Figure 6 Representative micrographs of kidney tissue stained with H&E (black arrows show glomerular degeneration; blue arrows show thickened basement membrane membranes).
Notes: (**A**) Natural control group, (**B**) model group, (**C**) rosiglitazone treatment group, (**D**) TB-II low-dose treatment group, (**E**) TB-II high-dose treatment group. The scale bar is 20 μm.
Abbreviations: TB-II, timosaponin B-II; H&E, hematoxylin and eosin.

Abnormal lipid metabolism also plays an important role in the pathogenesis of DN.[31] TC and TG are primary lipid metabolic factors, and the levels of TC and TG are typically increased in diabetic patients.[32] The results of the present study showed that the TC and TG levels were significantly increased in the alloxan-induced diabetic mice, suggesting that abnormal lipid metabolism is associated with DN. Surprisingly, the levels of TC and TG were significantly decreased at 4 weeks after TB-II treatment, indicating that TB-II could benefit diabetic mice via the regulation of abnormal lipid metabolism. Metformin, an antidiabetic drug, improves lipid metabolism and attenuates lipid peroxidation via enhancing insulin sensitivity.[33] Compared with metformin, TB-II might undergo a similar mechanism to regulate abnormal lipid metabolism via enhancing insulin sensitivity.

Previous studies have indicated that inflammatory cytokines, such as TNF-α and IL-6, play an important role in the development and progression of DN.[34–36] The levels of TNF-a, and IL-6 were increased in the renal tissues of diabetic mice, and this effect was critically dependent on the activation of NF-κB. NF-κB interacted with IκBα, thereby preventing sequestration in the cytoplasm. Once simulated, IκBα is phosphorylated and degraded through the IκB kinase complex, facilitating the translocation of NF-κB from the cytosol to the nucleus, where this protein binds to the promoter region of target genes.[37] In the present study, TB-II markedly decreased TNF-α and IL-6 concentrations in diabetic mice. In addition, we observed that TB-II inhibited IκBα phosphorylation and alloxan-induced nuclear translocation, suggesting that the attenuated diabetic renal injury observed after TB-II treatment might occur through the inhibition of inflammatory factors in NF-κB signaling pathways.

The dysregulation of the mTOR pathway results in metabolic disorders, leading to DN.[38] Several studies have suggested that the mTOR signaling pathway plays an important pathogenic role in DN.[39–41] The activation of mTOR signaling leads to renal hypertrophy during the early stages of diabetes.[42] In the present study, the data indicated that TB-II significantly inhibited mTOR phosphorylation at the doses of 100 mg/kg, suggesting that TB-II ameliorated diabetic renal injury through

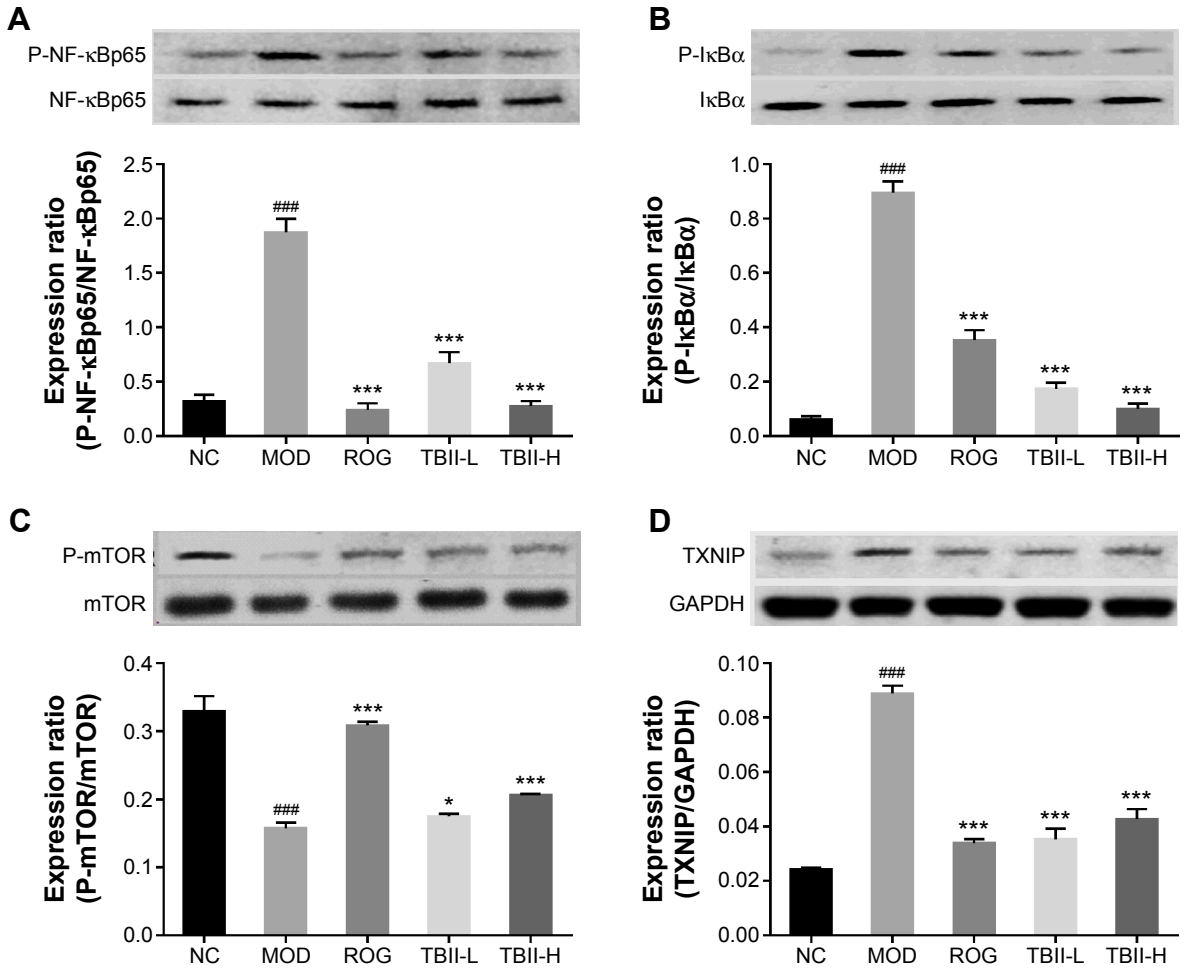

Figure 7 Effects of TB-II on NF-κB (**A**), IκBα (**B**), mTOR (**C**), and TXNIP (**D**), expression in renal tissues. The protein expression in renal cells suspension was visualized.
Notes: ###$P<0.001$ vs the normal control group; *$P<0.05$, ***$P<0.001$ vs the diabetic control group.
Abbreviations: GAPDH, glyceraldehyde 3-phosphate dehydrogenase; IκBα, inhibitory kappa B alpha; MOD, model group; mTOR, mammalian target of rapamycin; NC, natural control group; NF-κB, nuclear transcription factor-κB; ROG, rosiglitazone treatment group; TBII-L, TB-II low-dose treatment group; TBII-H, TB-II high-dose treatment group; TXNIP, thioredoxin-interacting protein; TB-II, timosaponin B-II.

the inhibition of the mTOR signaling pathway. A recent study also showed that TXNIP plays a key role in defective glucose homeostasis. TXNIP also inhibits glucose uptake, and TXNIP expression levels are consistently elevated in humans with Type 2 diabetes mellitus.[43] TXNIP promoted the β-cell death and controlled microRNA expression and insulin production, thereby contributing to diabetes progression. The results of the present study indicated that TB-II significantly decreases TXNIP expression in diabetic mice. Based on these data, it is likely that TB-II could represent a potential treatment for DN.

Conclusion

TB-II likely ameliorates diabetic renal injury through the regulation of NF-κB, mTOR, and TXNIP signaling pathways. Moreover, the antidiabetic mechanism of TB-II requires further investigation for the future development of an effective antidiabetic drug.

Acknowledgments

This work was supported by the Natural Science Foundation of Jiangsu Province (No BK20140674), the National Natural Science Foundation of China (Nos 81403080 and 81303223), and the Natural Science Research Project of Jiangsu Higher Education Institution (No 13KJB360012).

Disclosure

The authors report no conflicts of interest in this work.

References

1. Hajiaghaalipour F, Khalilpourfarshbafi M, Arya A. Modulation of glucose transporter protein by dietary flavonoids in type 2 diabetes mellitus. *Int J Biol Sci*. 2015;11(5):508–524.
2. Lontchi-Yimagou E, Sobngwi E, Matsha TE, Kengne AP. Diabetes mellitus and inflammation. *Curr Diab Rep*. 2013;13(3):435–444.
3. American Diabetes Association. Diagnosis and classification of diabetes mellitus. *Diabetes Care*. 2009;32(Suppl 1):S62–S67.

4. Guariguata L, Whiting DR, Hambleton I, Beagley J, Linnenkamp U, Shaw JE. Global estimates of diabetes prevalence for 2013 and projections for 2035. *Diabetes Res Clin Pract*. 2014;103(2):137–149.
5. Cao Z, Cooper ME. Pathogenesis of diabetic nephropathy. *J Diabetes Investig*. 2011;2(4):243–247.
6. Witzel II, Jelinek HF, Khalaf K, Lee S, Khandoker AH, Alsafar H. Identifying common genetic risk factors of diabetic neuropathies. *Front Endocrinol (Lausanne)*. 2015;6:88.
7. Hendrick AM, Gibson MV, Kulshreshtha A. Diabetic retinopathy. *Prim Care*. 2015;42(3):451–464.
8. Al-Malki AL. Assessment of urinary osteopontin in association with podocyte for early predication of nephropathy in diabetic patients. *Dis Markers*. 2014;2014(1):251–278.
9. Lim AK, Tesch GH. Inflammation in diabetic nephropathy. *Mediators Inflamm*. 2012;2012:146–154.
10. Shoelson SE, Lee J, Yuan M. Inflammation and the IKK beta/I kappa B/NF-kappa B axis in obesity- and diet-induced insulin resistance. *Int J Obes Relat Metab Disord*. 2003;27(Suppl 3):S49–S52.
11. Tan CY, Weier Q, Zhang Y, Cox AJ, Kelly DJ, Langham RG. Thioredoxin-interacting protein: a potential therapeutic target for treatment of progressive fibrosis in diabetic nephropathy. *Nephron*. 2015; 129(2):109–127.
12. Ya-li W, Yuan-yuan W, Di L, Jin-lin W, Dong-fang L. Relationship between TXNIP, diabetes and its complications. *Int J Endocrinol Metab*. 2013;33(1):53–55.
13. Godel M, Hartleben B, Herbach N, et al. Role of mTOR in podocyte function and diabetic nephropathy in humans and mice. *J Clin Invest*. 2011;121(6):2197–2209.
14. Wang Y, Dan Y, Yang D, et al. The genus *Anemarrhena* Bunge: a review on ethnopharmacology, phytochemistry and pharmacology. *J Ethnopharmacol*. 2014;153(1):42–60.
15. Xing JI, Feng YF. Advances in studies on saponins in *Anemarrhena asphodeloides*. *Chin Tradit Herbal Drug*. 2010;41(4):12–15.
16. Li TJ, Qiu Y, Yang PY, Rui YC, Chen WS. Timosaponin B-II improves memory and learning dysfunction induced by cerebral ischemia in rats. *Neurosci Lett*. 2007;421(2):147–151.
17. Mingzhu L, Zhiqian Z, Jia Y, Chen W, Zhonghat H, Tiejun L. Study on the effect and mechanisms of timosaponin B-II on antidepressant. *J Pharm Pract*. 2010;01(4):283–287.
18. Lu WQ, Qiu Y, Li TJ, Tao X, Sun LN, Chen WS. Timosaponin B-II inhibits pro-inflammatory cytokine induction by lipopolysaccharide in BV2 cells. *Arch Pharm Res*. 2009;32(9):1301–1308.
19. Deng XY, Chen JJ, Li HY, Ma ZQ, Ma SP, Fu Q. Cardioprotective effects of timosaponin B II from *Anemarrhenae asphodeloides* Bge on isoproterenol-induced myocardial infarction in rats. *Chem Biol Interact*. 2015;240:22–28.
20. Lu WQ, Qiu Y, Li TJ, Tao X, Sun LN, Chen WS. Antiplatelet and antithrombotic activities of timosaponin B-II, an extract of *Anemarrhena asphodeloides*. *Clin Exp Pharmacol Physiol*. 2011;38(7):430–434.
21. Nakashima N, Kimura I, Kimura M, Matsuura H. Isolation of pseudoprototimosaponin AIII from rhizomes of *Anemarrhena asphodeloides* and its hypoglycemic activity in streptozotocin-induced diabetic mice. *J Nat Prod*. 1993;56(3):345–350.
22. Guo C, Han F, Zhang C, Xiao W, Yang Z. Protective effects of oxymatrine on experimental diabetic nephropathy. *Planta Med*. 2014;80(4): 269–276.
23. Okwa IB, Akindele AJ, Agbaje EO, Oshinuga OT, Anunobi CC, Adeyemi OO. Effect of subclinical, clinical and supraclinical doses of calcium channel blockers on models of drug-induced hepatotoxicity in rats. *EXCLI J*. 2013;12:231–250.
24. Lenzen S, Panten U. Alloxan: history and mechanism of action. *Diabetologia*. 1988;31(6):337–342.
25. Evan A, Mong S, Connors B, Aronoff G, Luft F. The effect of alloxan and alloxan-induced diabetes on the kidney. *Anat Rec*. 1984;208(1): 33–47.
26. Zhou X, You S. Rosiglitazone inhibits hepatic insulin resistance induced by chronic pancreatitis and IKK-beta/NF-kappaB expression in liver. *Pancreas*. 2014;43(8):1291–1298.
27. Mohanty P, Aljada A, Ghanim H, et al. Evidence for a potent antiinflammatory effect of rosiglitazone. *J Clin Endocrinol Metab*. 2004;89(6): 2728–2735.
28. Kai-lin W, Gan-xiong L. Research progress of the relationship between serum uric acid level and diabetic nephropathy in patients with type 2 diabetes mellitus. *Hainan Med J*. 2013;24(4):576–578.
29. Siu YP, Leung KT, Tong MK, Kwan TH. Use of allopurinol in slowing the progression of renal disease through its ability to lower serum uric acid level. *Am J Kidney Dis*. 2006;47(1):51–59.
30. Chen GL, Wei W, Xu SY. Effect and mechanism of total saponin of Dioscorea on animal experimental hyperuricemia. *Am J Chin Med*. 2006;34(1):77–85.
31. Herman-Edelstein M, Scherzer P, Tobar A, Levi M, Gafter U. Altered renal lipid metabolism and renal lipid accumulation in human diabetic nephropathy. *J Lipid Res*. 2014;55(3):561–572.
32. Chen T, Gao J, Xiang P, et al. Protective effect of platycodin D on liver injury in alloxan-induced diabetic mice via regulation of Treg/Th17 balance. *Int Immunopharmacol*. 2015;26(2):338–348.
33. Anurag P, Anuradha CV. Metformin improves lipid metabolism and attenuates lipid peroxidation in high fructose-fed rats. *Diab Obes Metab*. 2002;4(1):36–42.
34. Mora C, Navarro JF. Inflammation and diabetic nephropathy. *Curr Diab Rep*. 2006;6(6):463–468.
35. Mora C, Navarro JF. The role of inflammation as a pathogenic factor in the development of renal disease in diabetes. *Curr Diab Rep*. 2005; 5(6):399–401.
36. Donath MY, Shoelson SE. Type 2 diabetes as an inflammatory disease. *Nat Rev Immunol*. 2011;11(2):98–107.
37. Karin M, Delhase M. The I kappa B kinase (IKK) and NF-kappa B: key elements of proinflammatory signalling. *Semin Immunol*. 2000; 12(1):85–98.
38. Inoki K. Role of TSC-mTOR pathway in diabetic nephropathy. *Diab Res Clin Pract*. 2008;82(Suppl 1):S59–S62.
39. Lloberas N, Cruzado JM, Franquesa M, et al. Mammalian target of rapamycin pathway blockade slows progression of diabetic kidney disease in rats. *J Am Soc Nephrol*. 2006;17(5):1395–1404.
40. Sataranatarajan K, Mariappan MM, Lee MJ, et al. Regulation of elongation phase of mRNA translation in diabetic nephropathy: amelioration by rapamycin. *Am J Pathol*. 2007;171(6):1733–1742.
41. Yang Y, Wang J, Qin L, et al. Rapamycin prevents early steps of the development of diabetic nephropathy in rats. *Am J Nephrol*. 2007;27(5): 495–502.
42. Sakaguchi M, Isono M, Isshiki K, Sugimoto T, Koya D, Kashiwagi A. Inhibition of mTOR signaling with rapamycin attenuates renal hypertrophy in the early diabetic mice. *Biochem Biophys Res Commun*. 2006; 340(1):296–301.
43. Stoltzman CA, Peterson CW, Breen KT, Muoio DM, Billin AN, Ayer DE. Glucose sensing by MondoA:Mlx complexes: a role for hexokinases and direct regulation of thioredoxin-interacting protein expression. *Proc Natl Acad Sci U S A*. 2008;105(19):6912–6917.

Supplementary materials

Timosaponin B-II

White amorphous powder; The molecular formula of TB-II was $C_{45}H_{76}O_{19}$ with a cluster ion peak at m/z 919.5013 $[M–H]^-$ ^{1}H-NMR (400 MHz, pyridine-d5) δ 5.27 (d, J=7.7 Hz, 1H), 4.97 (d, J=7.6 Hz, 1H), 4.76 (d, J=7.7 Hz, 1H), 0.99 (1H, d, J=5.9 Hz), 0.93 (s, 3H), 0.82 (s, 3H). ^{13}C-NMR (100 MHz, pyridine-d5; Table S1).

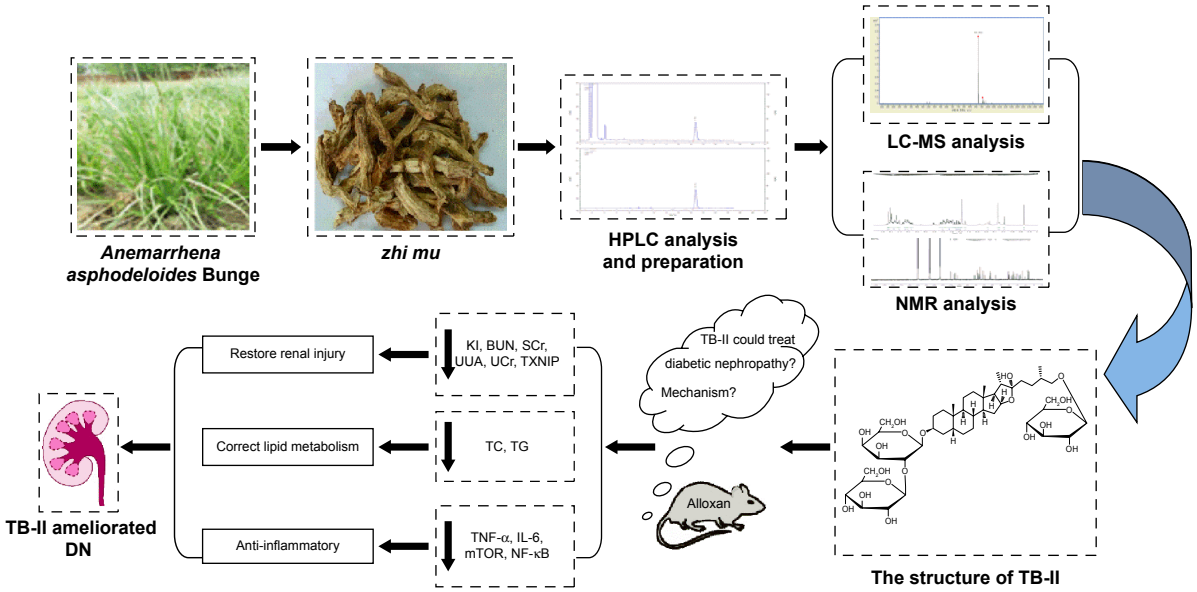

Figure S1 The work flow of the present study.
Abbreviations: BUN, blood urea nitrogen; DN, diabetic nephropathy; HPLC, high-performance liquid chromatograph; IL-6, interleukin-6; LC-MS, liquid chromatography-mass spectrometry; KI, kidney index; mTOR, mammalian target of rapamycin; NF-κB, nuclear transcription factor-κB; NMR, nuclear magnetic resonance; SCr, serum creatinine; TB-II, timosaponin B-II; TC, total cholesterol; TG, triglycerides; TNF-α, tumor necrosis factor-α; TXNIP, thioredoxin-interacting protein; UCr, urine creatinine; UUA, urinary uric acid.

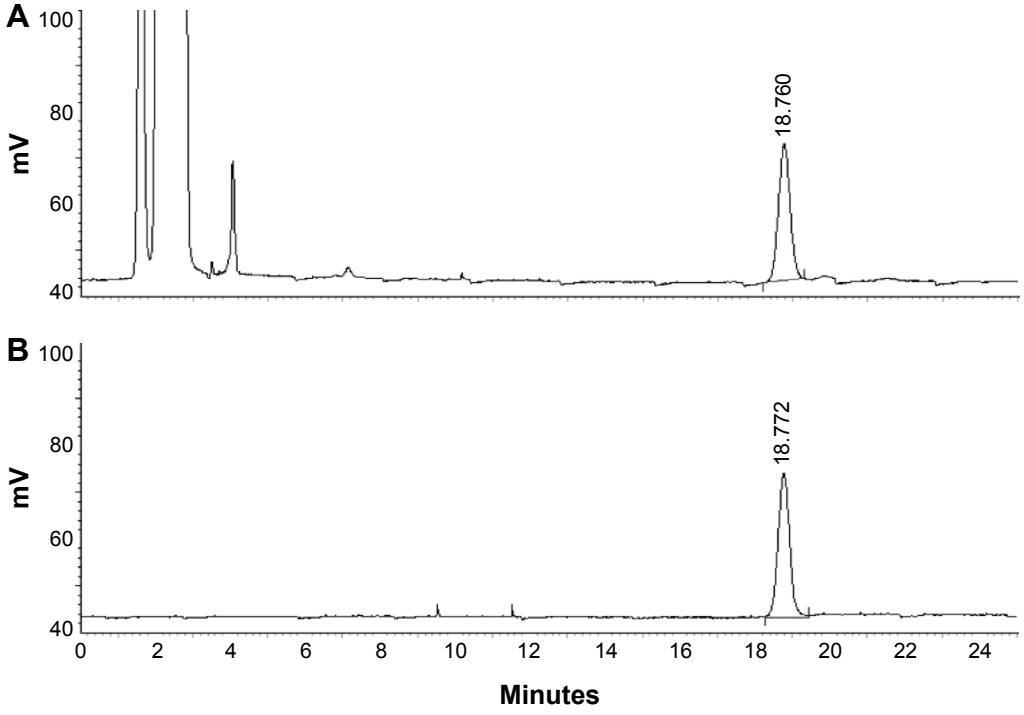

Figure S2 Liquid chromatogram of the rhizomes of *Anemarrhena asphodeloides* Bunge (**A**). Liquid chromatogram of purified TB-II (**B**).
Abbreviation: TB-II, timosaponin B-II.

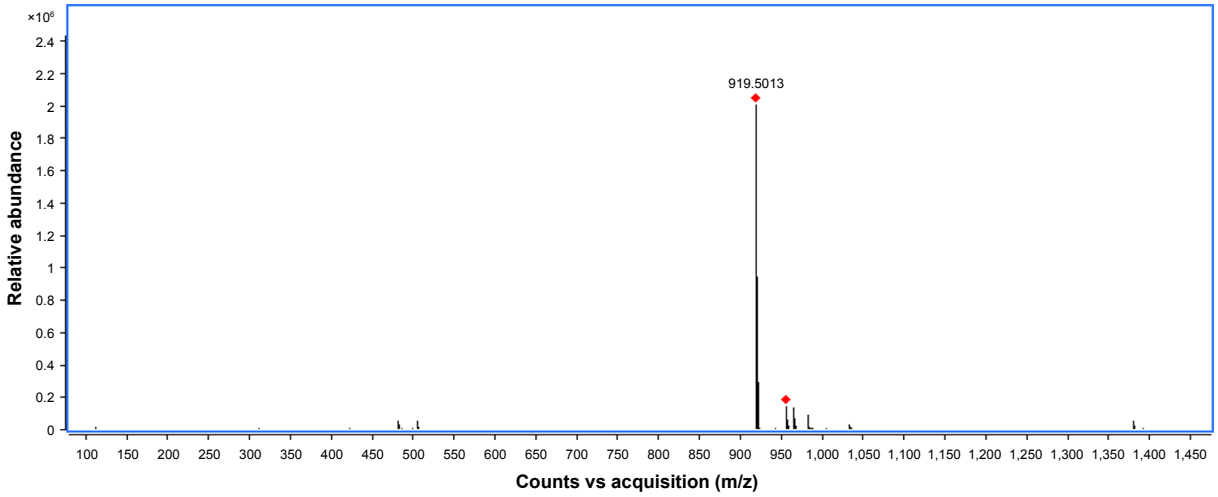

Figure S3 The negative ion electrospray ionization mass spectrometry (ESI-MS) of TB-II (negative-ESI-MS).
Abbreviation: TB-II, timosaponin B-II.

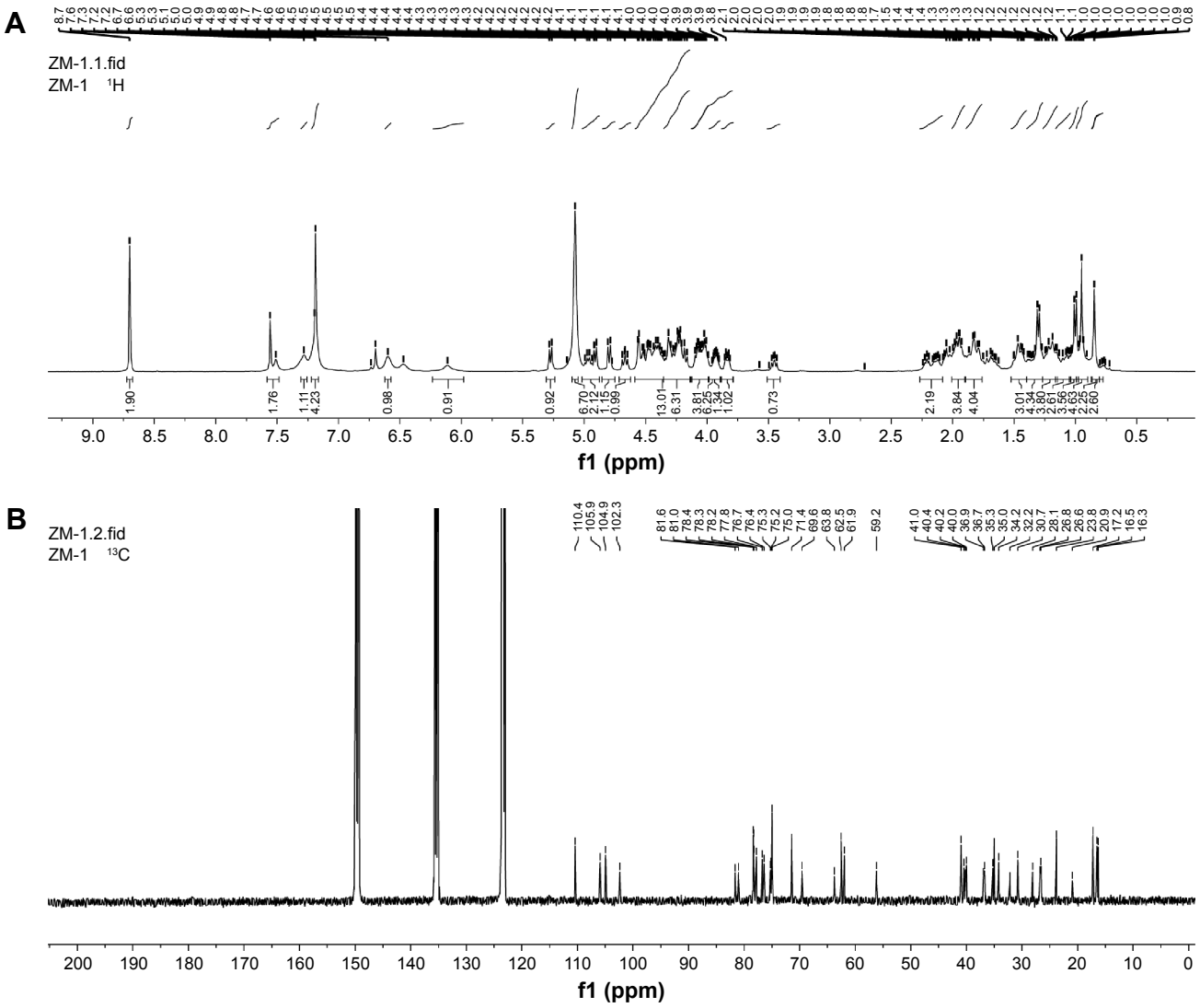

Figure S4 ^{1}H-NMR spectrum of TB-II (400 MHz, pyridine-d5; **A**); ^{13}C-NMR spectrum of TB-II (100 MHz, pyridine-d5; **B**).
Abbreviations: TB-II, timosaponin B-II; NMR, nuclear magnetic resonance; ppm, parts per million.

Table S1 ^{13}C-NMR spectroscopic data of TB-II (pyridine-d5, 100 MHz)

Position	TB-II	Position	TB-II	Position	TB-II
1	30.7	16	81.0	4	69.6
2	26.8	17	63.8	5	76.4
3	75.0	18	16.5	6	61.9
4	30.7	19	23.8	Glc″-1	105.9
5	36.7	20	40.4	2	75.3
6	26.8	21	16.3	3	77.8
7	26.6	22	110.4	4	71.4
8	35.2	23	36.9	5	78.2
9	40.0	24	28.1	6	62.5
10	35.0	25	34.2	Glc‴-1	104.9
11	20.9	26	75.2	2	75.0
12	40.2	27	17.2	3	78.4
13	41.0	Gal′-1	102.3	4	71.4
14	56.2	2	81.6	5	78.3
15	32.2	3	76.7	6	62.5

Abbreviations: TB-II, timosaponin B-II; NMR, nuclear magnetic resonance.